Experimental study of the Neumann and Dirichlet boundary conditions in two-dimensional electrostatic problems

Salvador Gil[a)]
Departamento de Física, Universidad de Buenos Aires, Argentina and Escuela de Ciencia y Tecnología de la Universidad Nacional de San Martín, Buenos Aires, Argentina

Martín Eduardo Saleta[b)] and Dina Tobia[c)]
Departamento de Física, Universidad de Buenos Aires, Argentina

(Received 9 April 2002; accepted 31 July 2002)

We present the results of an experimental study of the implications of the Neumann and Dirichlet boundary conditions on the solution of two-dimensional electrostatic problems. The experimental setup is simple and low cost. The experimental results are compared with theoretical expectations using a spreadsheet program to solve Laplace's equation with the appropriate boundary conditions. Excellent agreement is found between the experimental results and the calculations. The simplicity of the experiment and of the theoretical interpretation makes this experiment accessible to beginning students. © *2002 American Association of Physics Teachers.*
[DOI: 10.1119/1.1509418]

I. INTRODUCTION

The study of the solution of Laplace's equation with different types of boundary conditions is one of the most fundamental topics in intermediate and advanced courses on electromagnetism. In particular, the study of Neumann and Dirichlet boundary conditions is often presented in advanced courses.[1,2] Nonetheless, there is a relative scarcity of published experiments that illustrate their implication in practical situations and are suitable for use in teaching laboratories.

We present an experimental study of a two-dimensional electrostatic problem that clearly illustrates the importance of the Neumann and Dirichlet boundary conditions. Furthermore, the experimental results can be readily compared quantitatively with the numerical solution of Laplace's equation obtained by the relaxation method with the appropriate boundary conditions implemented in a spreadsheet.[3–6] The simplicity of the experiment and the technique for obtaining the solutions of Laplace's equation with different types of boundary conditions makes it possible to include these important topics earlier in the curricula.

The experimental setup we employ in our study of the field lines and equipotential surfaces is a dipolar configuration consisting of two electrodes immersed in a conducting media, distilled water in our case, which is contained in a rectangular basin. Typically, the conductivity, σ, of the water used ranged between 10^{-4} to $10^{-3}\ \Omega^{-1}\,\mathrm{m}^{-1}$. To prevent electrolysis, which would alter the chemical properties of the media over time, alternating current is used, with frequency, f, in the range of 50 Hz to 1 kHz. In this way the effective potential distribution does not change with time and hence is stationary. At the chosen frequencies, λ, the wavelength associated with the electromagnetic field is several hundred kilometers ($\lambda = c/nf \approx 10^6$ m, where c is the speed of light in vacuum and $n^2 = k$ is the dielectric constant of the liquid at the corresponding frequency). Because the wavelength is much larger than the linear dimensions of the experimental setup, the electric field configuration is essentially quasistatic and equivalent to the electrostatic case. Also, because the rate of change of the applied field is slow compared to the typical relaxation time of the media,[2,3] $\tau_r = k\varepsilon_0/\sigma$ ($\tau_r \sim 10^{-6}$ s), at each instant of time the potential distribution is the same as the electrostatic distribution. However, it changes with time at the applied alternating frequency.

Because we are considering stationary conditions ($1/f \gg \tau_r$), we have that $J = \sigma E$ at all times, where σ is the conductivity of the liquid media and J is the current density. Also the net charge density in the liquid is negligible, $\rho \approx 0$, and therefore the equation of continuity becomes

$$\boldsymbol{\nabla}\cdot(\sigma\mathbf{E}) = 0. \tag{1}$$

For quasistatic conditions, we have $\boldsymbol{\nabla}\times\mathbf{E} = 0$ and $\mathbf{E} = -\boldsymbol{\nabla}V$. Therefore

$$\boldsymbol{\nabla}\cdot(\sigma\boldsymbol{\nabla}V) = \sigma\boldsymbol{\nabla}^2 V = 0, \tag{2}$$

and the potential V satisfies Laplace's equation

$$\boldsymbol{\nabla}^2 V = 0. \tag{3}$$

A similar result can be obtained from the wave equation for the scalar potential ϕ,[1,3]

$$\boldsymbol{\nabla}^2\phi - \frac{1}{c^2}\frac{\partial^2\phi}{\partial t^2} = 0. \tag{4}$$

If $\phi(r,t) = V(r)\exp(i\omega t)$, where $\omega = 2\pi f$, then in the long wavelength approximation, that is, λ much larger than the characteristic length of the system, we have

$$\boldsymbol{\nabla}^2 V = \frac{1}{\bar{\lambda}^2}V \to 0 \quad \text{if } \bar{\lambda} = \frac{\lambda}{2\pi} \to \infty. \tag{5}$$

Because the basin that contains the water is nonconducting (acrylic), the current density J in the water can only flow parallel to the walls of the container. Therefore the perpendicular component of the current J is zero at the surface of a nonconducting wall. On these surfaces we have

$$\frac{\partial V}{\partial n} = 0, \tag{6}$$

where n indicates the direction perpendicular to the surface. This type of constraint on the potential is known as a Neumann boundary condition.[1]

On the other hand, if we have a water–metal interface, then because of the continuity equation,

$$J_{1n}=J_{2n}, \tag{7}$$

we have

$$\sigma_1 E_{1n}=\sigma_2 E_{2n}. \tag{8}$$

Here 1 and 2 refer to the liquid media and the metal, respectively, and $n(p)$ indicates the normal (parallel) component of the electric field. Because the conductivity of the metal $[\sigma_{\mathrm{Al}}\approx 3.7\times 10^7\ (\Omega\mathrm{m})^{-1}]$ is much larger than that of the liquid medium $[\sigma_{\mathrm{water}}\sim 10^{-3}(\Omega\mathrm{m})^{-1}]$, we find

$$\left(\frac{\sigma_1}{\sigma_2}\right)E_{1n}=E_{2n}\approx 0. \tag{9}$$

Therefore, we expect the electric field inside the conductor to be much smaller than the electric field in the water. In other words, the metal is essentially an equipotential volume. If we apply the Faraday induction law to the metal–liquid interface,[1,3] we obtain

$$E_{1p}=E_{2p}. \tag{10}$$

Because the metal is at a (almost) constant potential, $E_{1p}\approx 0$, and the electric field in the liquid is perpendicular to the water–metal interface. In summary, the metallic conductors constitute equipotential volumes, that is,

$$V_{\mathrm{cond}}=\text{constant}. \tag{11}$$

This type of constraint on the potential is known as the Dirichlet boundary condition.[1]

The experimental setup can be arranged to have a Dirichlet or a Neumann boundary condition on the edge of the basin by simply placing a conductor on the rim or leaving the nonconducting material uncovered. It is also possible to construct a combination of the two types of boundary conditions with the same setup.

II. NUMERICAL SOLUTION OF THE LAPLACE'S EQUATION IN TWO DIMENSIONS

There are several methods to solve Laplace's equation in two dimensions.[3,7] The numerical technique that we will use is the relaxation method[4–6,8] which can easily be implemented using almost any spreadsheet program.

$$\nabla^2 V(x,y)=\frac{\partial^2 V(x,y)}{\partial x^2}+\frac{\partial^2 V(x,y)}{\partial y^2}=0. \tag{12}$$

The relaxation technique in two dimensions has been extensively discussed in the literature,[3,5,6,8] and is an example of a finite difference method. It consists of dividing the region over which we wish to find the solution of Laplace's equation into a regular square mesh grid of dimension $h\times h$. In particular, for a rectangular region of dimensions $a\times b$, the interval of length a is divided into $n=a/h$ segments and the interval of length b is divided into $m=b/h$ segments. The center of each square is characterized by the index i $(1<i<n)$ and j $(1<j<m)$. For simplicity, we use the notation that (i,j) indicates the coordinates (x_i,y_j). The three point approximation is used for the second derivative

$$\frac{\partial^2 V(x_0,y_0)}{\partial x^2}\approx\frac{V(x_0+h,y_0)-2V(x_0,y_0)+V(x_0-h,y_0)}{h^2}. \tag{13}$$

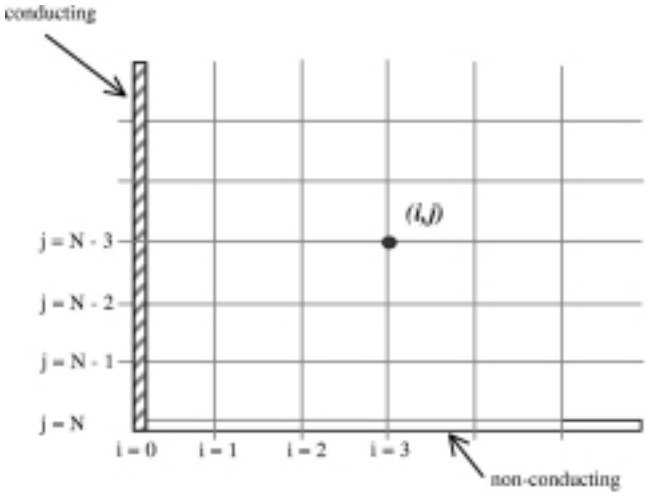

Fig. 1. Schematic representation of a lower corner of the basin, limited by a mixed boundary condition. The lower horizontal rim is nonconducting, and therefore satisfies the Neumann boundary condition, while the left vertical rim is metallic (conducting) and has been set to a potential V_0. Therefore this wall of the basin satisfies a Dirichlet boundary condition.

If we use the equivalent expression for $\partial^2 V(x_0,y_0)/\partial y^2$, it is easy to see that Eqs. (12) and (13) lead to

$$V(x_0,y_0)=\tfrac{1}{4}(V(x_0-h,y_0)+V(x_0+h,y_0)+V(x_0,y_0-h)+V(x_0,y_0+h)), \tag{14}$$

or in our simplified notation

$$V(i,j)=\tfrac{1}{4}(V(i-1,j)+V(i+1,j)+V(i,j-1)+V(i,j+1)). \tag{15}$$

The solution of Laplace's equation can be obtained by an iteration procedure that is repeated until the maximum relative change in the function $V(i,j)$ from one iteration to the

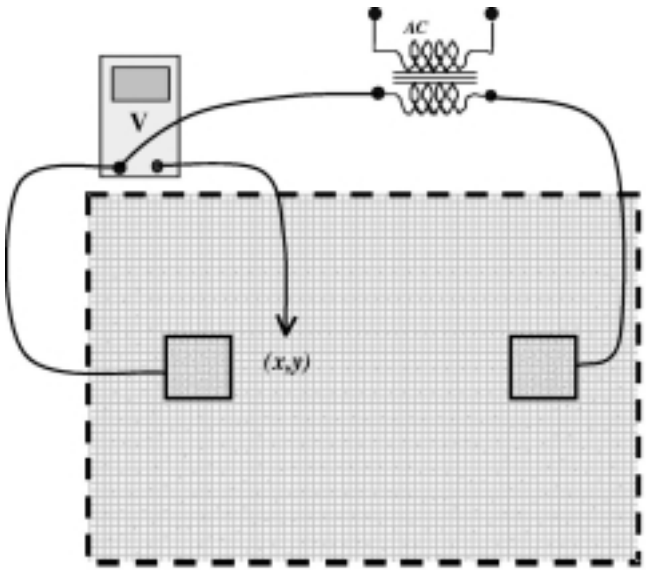

Fig. 2. Schematic diagram of the experimental setup. The dashed line around the rim of the basin indicates the different types of boundary conditions imposed on the system. If the vertical walls of the container are covered with a metallic (conducting) shim, we generate an equipotential surface on the rim, that is, Dirichlet boundary conditions are imposed. If the metallic shim is removed, Neumann boundary conditions are obtained.

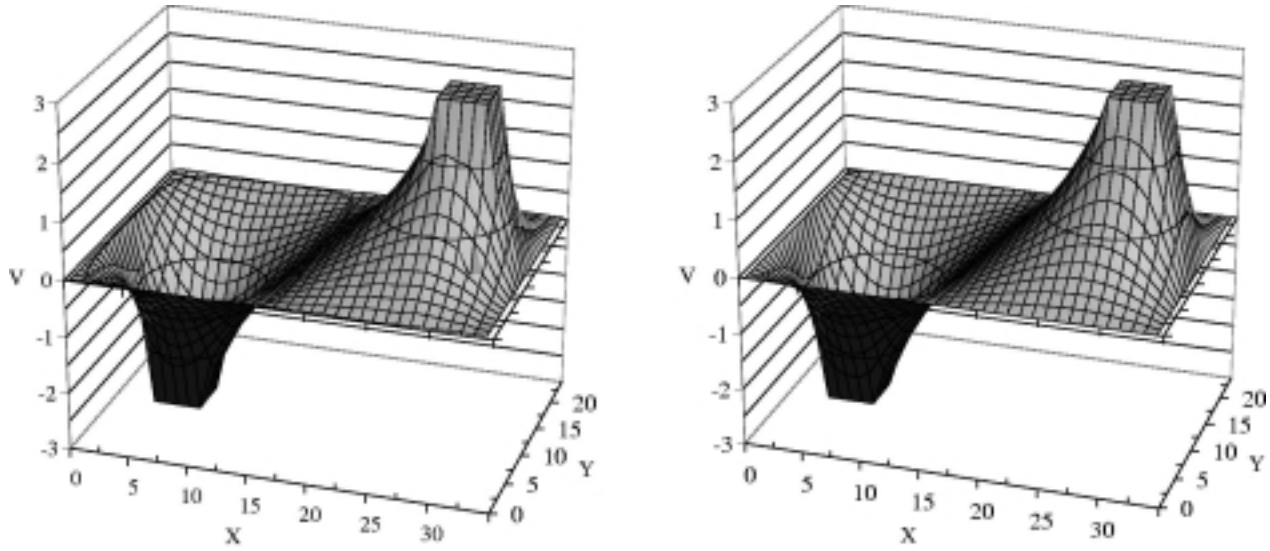

Fig. 3. Experimental (left-hand side) and theoretical (right-hand side) result of the potential for the Dirichlet boundary condition.

next is less than a prescribed tolerance of t. In our case we have chosen $t=0.001$. The boundary conditions are satisfied by requiring that on the surface of the conductor (Dirichlet boundary condition), characterized by $i=0$ in Fig. 1, the potential is set to a constant value, determined by the nature of the problem. Similarly, on the surface of a nonconducting material we require that

$$\frac{\partial V}{\partial n}=0, \tag{16}$$

that is, the Neumann boundary condition.

To illustrate how this technique can be implemented in a spreadsheet program, each mesh region (i,j) is represented by a corresponding cell in the spreadsheet where the value is the potential $V(i,j)$ at each point. As an example of the way that the boundary conditions are satisfied, let us assume that a given corner of the problem is limited on the left by a conducting electrode at a potential V_0 along the y axis (Dirichlet boundary condition), characterized by $i=0$ in Fig. 1, and a nonconducting wall on the lower horizontal axis (Neumann boundary condition), characterized by $j=N$ in Fig. 1. The value of any point in the mesh that is not on the boundary is obtained using Eq. (15). Those points that belong to a Dirichlet boundary are held to the applied potential V_0, that is

$$V(i=0,j)=V_0. \tag{17}$$

The Neumann boundary condition in this example is satisfied by requiring

$$V(i,j=N)=V(i,j=N-1), \tag{18}$$

where $V(i,j=N-1)$ is calculated using Eq. (15). The spreadsheets developed for this study are available and can be downloaded.[9]

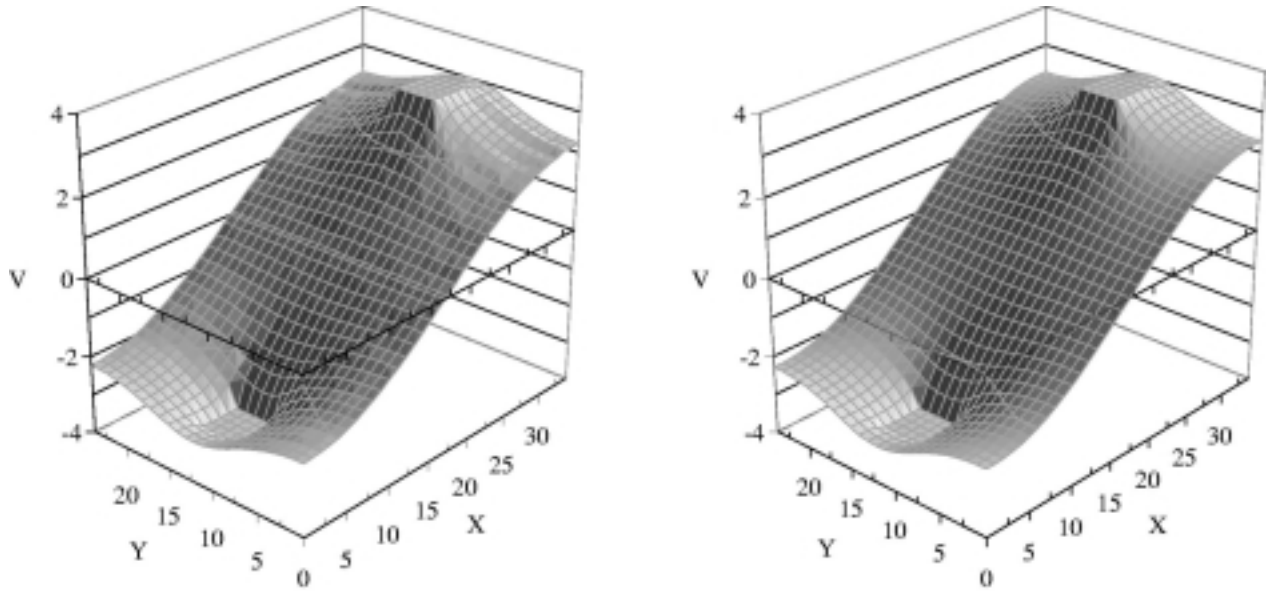

Fig. 4. Experimental (left-hand side) and theoretical (right-hand side) result of the potential for the Neumann boundary condition.

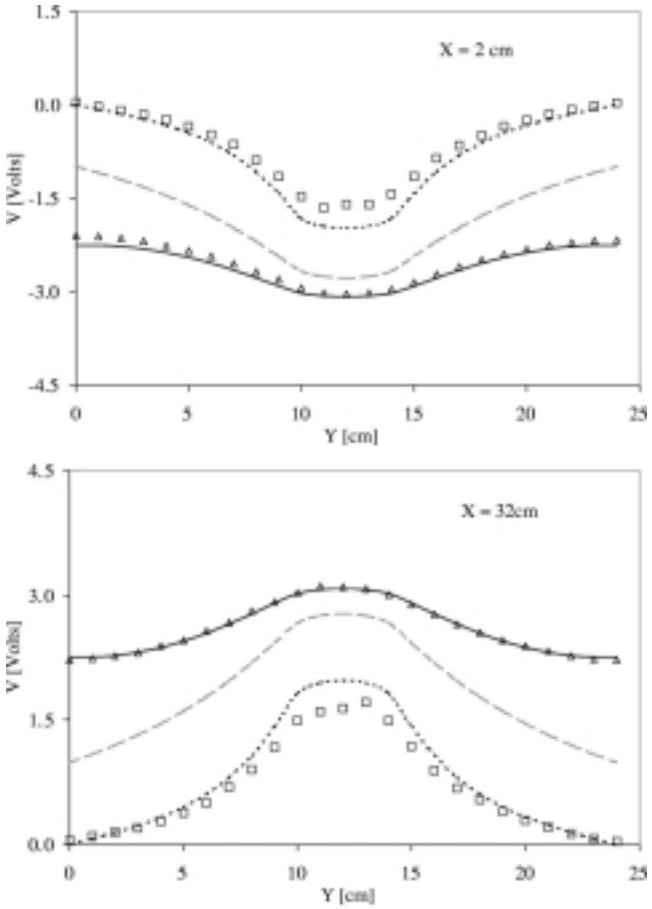

Fig. 5. Comparison of the potential as a function of the y coordinate for fixed values of $x=2$ cm and $x=32$, for both the Dirichlet and Neumann boundary conditions. The square symbols indicate the experimental result for the case of Dirichlet boundary condition and the triangular symbols indicate the Neumann boundary condition. The dotted curve is the prediction of the relaxation technique using the Dirichlet boundary condition, and the solid curve is the corresponding solution for the Neumann boundary condition. The dashed curve corresponds to the solution, ignoring the rim, that is, when the only requirement is that $V\rightarrow 0$ as any of the coordinates approaches infinity.

Although the finite difference technique based on Eq. (15) is not the most efficient procedure for the convergence of the solution,[3,8] it is simple to understand by beginning students, and with current personal computers a reasonable matrix size of 100×200 cells can be iterated 1000 times in less than a second. Therefore, it is usually not important to resort to more sophisticated techniques, such as over-relaxation, that are not so straightforward to implement with a spreadsheet.

III. EXPERIMENT

The experimental setup adopted to study the electrostatic potential is illustrated schematically in Fig. 2, and is similar to the one used by other authors[7] in the past. It consists of a transparent rectangular acrylic tray, 24 cm$\times$34 cm and 2 cm in height, with millimetric paper attached to the bottom, allowing the rectangular coordinates of each point to be recorded. Two aluminum electrodes of different shapes are connected to the secondary of a transformer that provides an AC voltage of $V_{0,\mathrm{eff}}\approx 10$ V (effective) at 50 Hz. The acrylic basin is filled with distilled water to approximately 1 cm

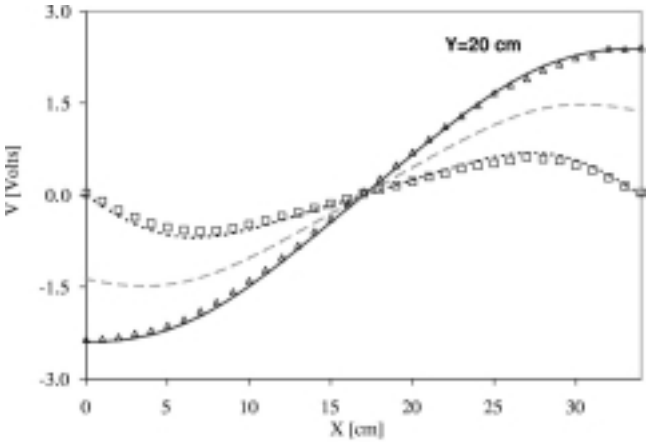

Fig. 6. Comparison of the potential as a function of the x coordinate for fixed value of $y=20$ cm, for both the Dirichlet and Neumann boundary conditions. The square symbols indicate the experimental result for the case of Dirichlet boundary condition, and the triangular symbols indicate the Neumann boundary condition. The dotted curve is the prediction of the relaxation technique using the Dirichlet boundary condition and the solid curve is the corresponding solution for the Neumann boundary condition. The dashed curve corresponds to the solution, ignoring the rim, that is, when the only requirement is that $V\rightarrow 0$ as any of the coordinates approaches infinity.

depth. A standard digital AC voltmeter is used to measure the potential at each point of the basin relative to one of the electrodes that is taken as a reference.

For the configuration indicated in Fig. 2, the equipotential line that bisects the axis that joins the center of the electrodes is at the effective potential $V_0/2$. By symmetry, this equipotential line extends to infinity. Therefore, if we want our potential to satisfy the usual convention of $V=0$ at infinity, we must normalize our measured values, V_{meas}, and take $V(x,y)=V_{\mathrm{meas}}(x,y)-V_0/2$. It should be emphasized that what is physically meaningful is the potential difference. In all the figures, the quoted potential has been normalized in this manner.

IV. RESULTS AND DISCUSSION

One of the most interesting advantages of the experimental setup used in this experiment is its versatility. It is very straightforward to study several types of configurations using different geometries for the electrodes as well as a variety of boundary conditions with only minor changes.

We first present our result for the geometry indicated in Fig. 2, using an electrically isolated metallic shim on the rim of the basin. This configuration corresponds to the Dirichlet boundary condition with $V=0$ ($V_{\mathrm{meas}}=V_0/2$) on the rim. The three-dimensional plot[10] on the left-hand side of Fig. 3 illustrates the experimental results, whereas the plot on the right-hand side corresponds to the solution of Laplace's equation, obtained by the relaxation method. The semiquantitative similarity between the two figures is clear.

To study the effect of changing the boundary conditions, we simply remove the metallic shim from the rim. The boundary conditions are now reduced to the Neumann boundary condition. The results are depicted in Fig. 4. On the left-hand side of this figure we have plotted the experimental results and on the right-hand side the theoretical prediction obtained by solving Laplace's equation. Again, the similarity between theory and experiment is clear. Further-

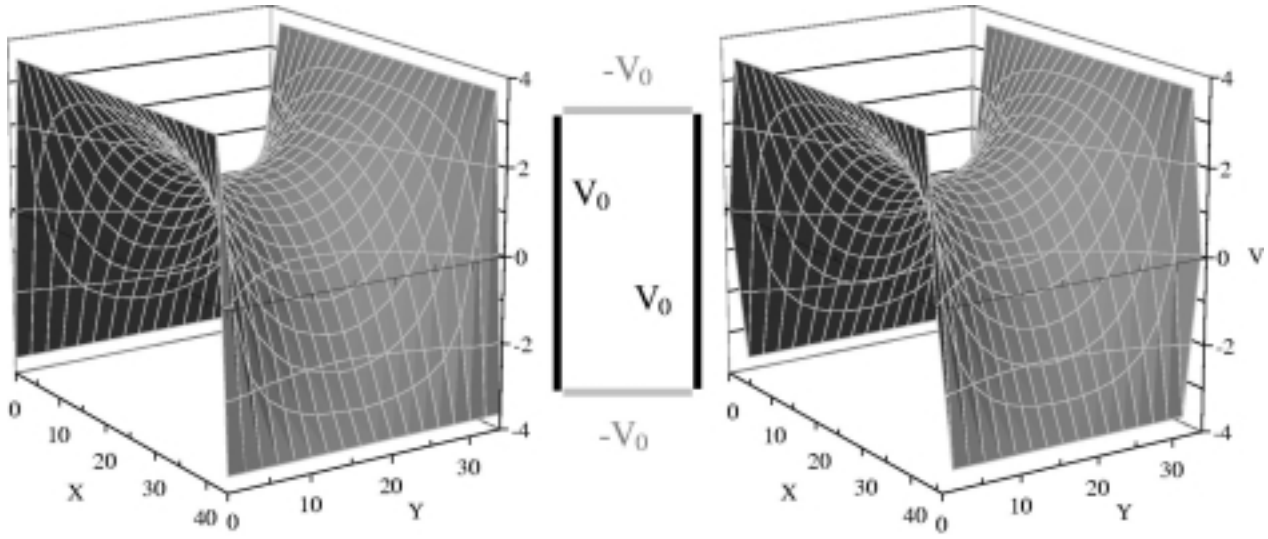

Fig. 7. A three-dimensional plot of the potential for the configuration shown at the center of this figure. On the left-hand side we show the experimental results and on the right-hand side we show the solution of Laplace's equation obtained by the relaxation method. The basin dimension used in this measurement was 35 cm×45 cm.

more, the difference in the result of both experiment and theory between Figs. 3 and 4 is very striking, making quite evident the physical implications of changing the boundary conditions of the system.

To make a more quantitative comparison of our results, we present two-dimensional plots in Figs. 5 and 6 of the variation of the potential along cuts parallel to the x and y axis. In particular, Fig. 5 illustrates the variation along an axis parallel to the y axis, at symmetrical distances from the electrodes ($x=2$ cm and $x=32$ cm) that correspond to an axis at about the mid-point between each electrode and the nearest wall. In Fig. 5 we have plotted the experimental results for both boundary conditions, together with the corresponding theoretical predictions. For comparison purposes, we have also plotted the theoretical results obtained by requiring that the potential $V=0$ at infinity. This situation is commonly made implicitly, when for instance we use as a model for the system of Fig. 2, the potential corresponding to a dipole configuration.[7] As is clear from Figs. 5 and 6, this last model of the potential does not agree with either of the configurations measured. Moreover, these figures illustrate the importance of the boundary condition in determining the potential of the system.

In Figs. 7 and 8 we present three-dimensional plots of the potentials obtained for two different arrangements of the electrodes. Figure 8 illustrates an interesting configuration of mixed boundary conditions, and Fig. 7 shows a configuration of electrodes that produces a typical quadrupole field that is very useful in situations that require focusing a beam of charged particles. The corresponding configuration is indicated at the center of these figures. On the left-hand side of each figure we present the experimental results and on the right-hand side we show the corresponding numerical solution of Laplace's equation. The similarities between theory and experiment are self-evident. Furthermore, they illustrate

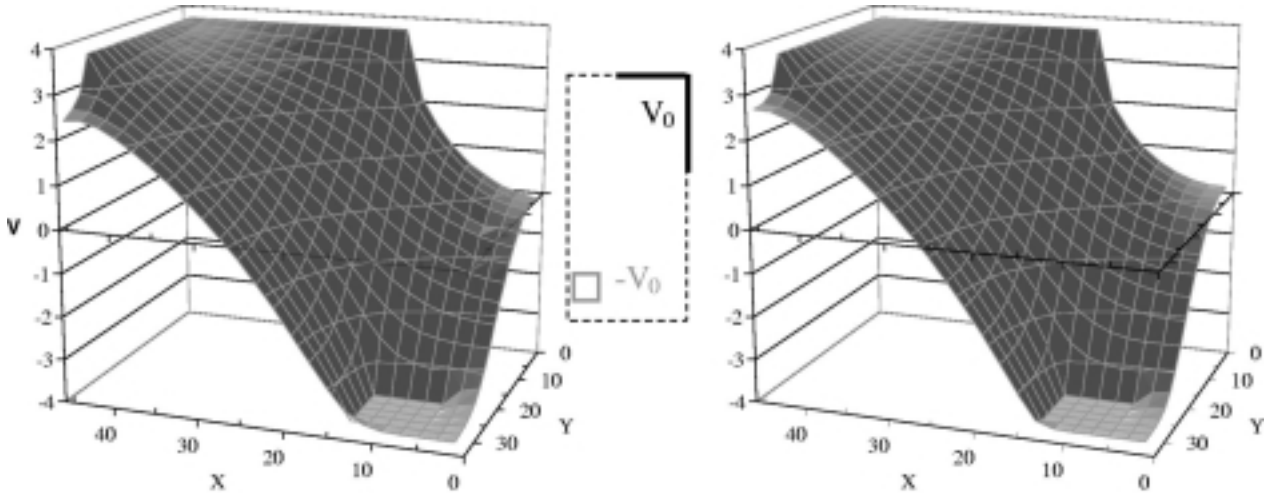

Fig. 8. Three-dimensional plot of the potential for the configuration shown at the center of this figure. On the left-hand side we show the experimental results and on the right-hand side we show the result of Laplace's equation obtained by the relaxation method. The basin dimension used in this measurement was 35 cm×45 cm.

the implication of the two types of boundary conditions on the potential configuration of the system.

V. CONCLUSIONS

The experiments discussed in this paper clearly show the importance of the Neumann and Dirichlet boundary conditions for the solutions of Laplace's equation for actual experimental situations. The experimental setup is very simple and very low cost. The experimental results can be quantitatively compared with realistic theoretical models. In particular, using the relaxation technique, the solutions for a whole variety of boundary conditions, Dirichlet, Neumann or mixed boundary conditions, can be obtained in a straightforward manner. In fact, arbitrary and complex boundary conditions as well as different shapes of electrodes can be implemented experimentally and solved numerically with the relaxation method. The results of the theoretical calculations are in good agreement with the experimental results.

An interesting laboratory project would be to ask students to measure the potential distribution of a dipolar configuration, similar to the ones depicted in Fig. 2, and compare the results with the prediction of a naive model of a dipolar configuration with $V=0$ at infinity. In particular we would ask the students to perform a quantitative comparison of the experimental results and the theoretical prediction along lines similar to those shown in Figs. 5 and 6. The two-dimensional plots would clearly indicate the shortcomings of the naive approach and the need to adequately account for the boundary conditions in order to obtain quantitative agreement with the theory. Finally, as an application and extension of solving potential problems, it would be interesting to ask students to devise their own set of boundary conditions, preferentially defining the boundary along segments parallel to the coordinate axis. This selection will simplify the solution of Laplace's equation using the relaxation method.

ACKNOWLEDGMENTS

We would like to acknowledge the valuable comments and suggestions made by Professor D. F. Mazzitelli, Professor C. Grosse, and Dr. A. Schwint.

[a]Electronic mail: sgil@df.uba.ar
[b]Electronic mail: msaleta@labs.df.uba.ar
[c]Electronic mail: dina@labs.df.uba.ar

[1]J. D. Jackson, *Classical Electrodynamics*, 3rd ed. (Wiley, New York, 1998), Chaps. 1 and 2.
[2]W. K. H. Panofsky and M. Philips, *Classical Electricity and Magnetism*, 2nd ed. (Addison-Wesley, Reading, MA, 1962), Chaps. 4 and 7.
[3]J. R. Reitz, J. R. Milford, and R. W. Christy, *Foundations of Electromagnetic Theory*, 4th ed. (Addison-Wesley, Reading, MA, 1993), Chaps. 3 and 7.
[4]M. Distancio and W. C. Harris, "Electrostatic problems? Relax!," Am. J. Phys. **47**, 440–444 (1979).
[5]B. Kaplan, "Comment on: Electrostatic problems? Relax!," Am. J. Phys. **50**, 964 (1982).
[6]W. MacDonald, "Discretization and truncation error in numerical solution of Laplace's equation," Am. J. Phys. **62**, 169–173 (1992).
[7]H. Murata and M. Sakuraoka, "Electrostatic potential on laboratory measurement experiment," Am. J. Phys. **48**, 763–766 (1980).
[8]B. P. Canova, "Laplace's equation in freshman physics," Am. J. Phys. **60**, 135–138 (1992).
[9](www.fisicarecreativa.com) Web site dedicated to experimental physics. It contains experimental projects using new technologies and reports of experiments performed by undergraduate students from different universities of Latin America.
[10]J. Horn, "Electrostatic landscape," Phys. Teach. **35**, 499–501 (1997).